Nat. Hazards Earth Syst. Sci. Discuss., 1, 4891–4924, 2013
www.nat-hazards-earth-syst-sci-discuss.net/1/4891/2013/
doi:10.5194/nhessd-1-4891-2013

Natural Hazards and Earth System Sciences
Discussions
Open Access

Modelling fire frequency and area burned across phytoclimatic regions in Spain using reanalysis data and the Canadian Fire Weather Index System

J. Bedia[1], **S. Herrera**[1], **and J. M. Gutiérrez**[2]

[1]Meteorology Group, Dept. Applied Mathematics and Computing Science, University of Cantabria, Avda. Los Castros s/n, 39005, Spain
[2]Meteorology Group, Institute of Physics of Cantabria, CSIC – University of Cantabria, Ed. Juan Jordá, Avda. Los Castros s/n, 39005, Spain

Received: 9 July 2013 – Accepted: 31 August 2013 – Published: 17 September 2013

Correspondence to: J. Bedia (bediaj@unican.es)

Published by Copernicus Publications on behalf of the European Geosciences Union.

Abstract

We develop fire occurrence and burned area models in peninsular Spain, an area of high variability in climate and fuel types, for the period 1990–2008. We based the analysis on a phytoclimatic classification aiming to the stratification of the territory into homogeneous units in terms of climatic and fuel type characteristics, allowing to test model performance under different climatic and fuel conditions. We used generalized linear models (GLM) and multivariate adaptive regression splines (MARS) as modelling algorithms and temperature, relative humidity, precipitation and wind speed, taken from the ERA-Interim reanalysis, as well as the components of the Canadian Forest Fire Weather Index (FWI) System as predictors. We also computed the standardized precipitation-evapotranspiration index (SPEI) as an additional predictor for the models of burned area.

We found two contrasting fire regimes in terms of area burned and number of fires: one characterized by a bimodal annual pattern, characterizing the Nemoral and Oro-boreal phytoclimatic types, and another one exhibiting an unimodal annual cycle, with the fire season concentrated in the summer months in the Mediterranean and Arid regions. The fire occurrence models attained good skill in most of the phytoclimatic zones considered, yielding in some zones notably high correlation coefficients between the observed and modelled inter–annual fire frequencies. Total area burned also exhibited a high dependence on the meteorological drivers, although their ability to reproduce the observed annual burned area time series was poor in most cases. We identified temperature and some FWI system components as the most important explanatory variables, and also SPEI in some of the burned area models, highlighting the adequacy of the FWI system for fire modelling applications and leaving the door opened to the development a more complex modelling framework based on these predictors. Furthermore, we demonstrate the potential usefulness of ERA-Interim reanalysis data for the reconstruction of historical fire-climate relationships at the scale of analysis. Fire frequency predictions may provide a preferable basis for past fire history reconstruction,

long-term monitoring and the assessment of future climate impacts on fire regimes across regions, posing several advantages over burned area as response variable.

1 Introduction

Fire is a global phenomenon that has a decisive influence on the ecosystems throughout the world (Bond et al., 2005; Beerling and Osborne, 2006) and as such, it must be regarded as an integral earth system process (Bowman et al., 2009). At the same time, wildfires are also the cause of important damages and economic losses in many fire-prone regions of the world, arising public concerns and requiring important economic efforts towards fire prevention, protection, suppression and restoration (Hardy, 2005; Barbati et al., 2010).

It is widely accepted that fire activity is strongly influenced by climate, although human activities and land uses are important factors in determining fire regimes (Pereira et al., 2005; Marlon et al., 2008). Climate exerts a direct control on fuels by determining fuel moisture and thus their flammability and indirect, by influencing the vegetation types and determining the primary productivity (i.e., the fuel structure). In the Mediterranean ecosystems, it has been shown the crucial role of fuels as drivers of the fire-climate relationships, for instance by determining the climatic threshold for switching to flammable conditions (Pausas and Paula, 2012). The relationships between antecedent climate and fire activity provides evidence on the close dependence of fuels on climate, which in turn have a direct influence on fire regime (Keeley, 2004; Pausas, 2004; Turco et al., 2012; Koutsias et al., 2012). Therefore, the understanding of the links between climate/weather, fuel characteristics and wildfires is of utmost importance for the effective implementation of management policies in fire-prone regions.

In this context, phytoclimatology is a scientific discipline focused on the establishment of links between natural vegetation and climatic types. As a result, the phytoclimatic classification provides a potentially useful framework for the characterization and analysis of wildfires, by identifying regions with homogeneous characteristics in terms of fuel types and climatic conditions. In peninsular Spain, the phytoclimatic regions defined (Allué, 1990) encompass a long gradient of bioclimatic conditions, ranging from the Atlantic area of influence, characterized by high precipitations and mild temperatures throughout the year, where potential vegetation is represented by broad-leaved deciduous forests, to the most arid areas of the South-east and the Ebro depression, where the natural vegetation potential corresponds to sparse formations of spiny shrubs. Following the conceptual framework introduced by Meyn et al. (2007) in the context of large, infrequent fires, the ecosystem types analysed range from the biomass-rich, rarely dry ecosystems characteristic of the Atlantic phytoclimatic types of northern Spain, to the biomass-poor, rarely wet ecosystems of the arid type. In the intermediate position of this gradient are located the fire-prone Mediterranean types, where fuel accumulation is important during one part of the year of high productivity, followed by a dry and warm season of high fire hazard.

In this study, we investigate the adequacy of the FWI system for the analysis of the fire history in Spain, as well as the practical applicability of reanalysis climate data – ERA-Interim – to this aim, following a previous study showing that this reanalysis product is adequate for the characterization of fire danger conditions in Iberia (Bedia et al., 2012). In addition, we analyse whether the phytoclimatic regions can be used as convenient generalization units for the development of accurate models of fire occurrence and burned area, by means of an spatial aggregation experiment. We determine the predictive ability of the models by applying cross–validation procedures, and calculate the contribution of the different candidate dependent variables to the total explained variance in order to ascertain which are the most important climatic controls of fires across phytoclimatic regions.

NHESSD
1, 4891–4924, 2013

2 Data and methods

2.1 Fire data

We extracted fire data from the National Wildfire Database of the Spanish Environmental Agency (Mérida et al., 2007). We selected all fires since 1990, the moment at which a rigorous fire reporting protocol with a normalized form started to be applied at a national level, thus ensuring the maximum homogeneity of the fire database across Spain. In total, the database stores more than 360 000 daily fire records across the whole country on a 10 km-resolution grid, describing a number of variables related to the fire events, including burnt area.

2.2 Phytoclimatic regions

The phytoclimatic regions used in this study were delimited according to the classification performed by Allué (1990) in Spain (Table 1), built upon meteorological data from the Spanish Meteorological Agency and the potential vegetation series elaborated by Rivas Martínez (1987). The resulting classification consists of 19 different subtypes of vegetation, each of them linked to characteristic climatic conditions, which are grouped in four general phytoclimatic types, then subdivided into more specific types. Due to the small area encompassed by some of the phytoclimatic zones, we made an aggregation of some of them with the neighbouring units, based on the spatial proximity and ecological affinity in terms of vegetation types. As a result, phytoclimatic types 2–3, 7–8, 10–11–12 and 13–14–15 were merged together for the analyses. In addition, due to the very low fire numbers in the oro-boreal phytoclimatic region, the corresponding types were merged together with class 13–14–15 (Fig. 1). Similarly, type 1 was restricted to a very small coastal Mediterranean area, falling out from the 25km-resolution land mask applied, and therefore it was discarded from the analysis.

NHESSD
1, 4891–4924, 2013

2.3 Climate data

We obtained climate data from the ERA-Interim reanalysis, produced by the European Centre for Medium-Range Weather Forecasts in collaboration with many institutions (Dee et al., 2011). The performance of different reanalysis products in the Iberian Peninsula and further details on their use for fire danger estimation are described in (Bedia et al., 2012). The main advantages of reanalysis data are the wide geographical coverage and the homogeneity of the time series provided. In addition, reanalysis products generally provide a large number of variables, including those needed at surface level for the reconstruction of FWI series, some of them (in particular wind speed and humidity) difficult to obtain from observational datasets over large areas.

2.4 The Canadian Forest Fire Weather Index System

The Fire Weather Index (FWI) System consists of six components rating the effects of fuel moisture content and wind on a daily basis, based on various factors related to potential fire behaviour (van Wagner, 1987; Stocks et al., 1989). The first three components, referred to as the Fine Fuel Moisture Code (FFMC), the Duff Moisture Code (DMC) and the Drought Code (DC), rate the average moisture content of different soil layers, respectively fine surface litter, decomposing litter, and organic layers. Wind effects are then added to FFMC to form the Initial Spread Index (ISI), which is an indicator of the rate of fire spread. The remaining two fuel moisture codes (DMC and DC) are combined to produce the Build Up Index (BUI), which rates the total amount of fuel available for combustion. BUI is finally combined with ISI to produce the Fire Weather Index (FWI), a dimensionless index rating the potential fire line intensity given the meteorological conditions at noon local standard time in a reference fuel type (mature pine stands). The FWI System uses as input four meteorological variables: daily accumulated precipitation, instantaneous wind speed, instantaneous humidity and instantaneous temperature. Further details on the procedure for FWI system calculation from reanalysis outputs are described in the companion paper (Bedia et al., 2012).

NHESSD
1, 4891–4924, 2013

2.5 Drought indices

Drought is an important factor related to wildfire occurrence and magnitude (see e.g. Pereira et al., 2005; Littell et al., 2009; Meyn et al., 2010). Unlike the previous daily fire danger indices, droughts are climatic phenomena difficult to quantify in terms of intensity, magnitude, duration and spatial extent, partly because there is no a straightforward manner to identify their onset, duration and end (Vicente-Serrano et al., 2010). A number of specific indices have been developed in order to quantify and properly describe drought episodes, and in this study we have included two of them: The Standardized Precipitation Index (SPI) and the standardized precipitation-evapotranspiration index (SPEI). Unlike other popular drought indices, both SPI and SPEI account for the widely accepted multi-scalar nature of droughts (see e.g. McKee et al., 1993). Both indices are calculated on a monthly basis, and therefore they have been only tested as predictors in the burned area models.

SPI is an index based on the probability of recording a given amount of precipitation at a specific point and can represent precipitation dynamics over user-selected time frames (McKee et al., 1993). However, SPI does not take into account temperature, and thus may present important deviations from the true water deficits derived from evapotranspiration. As a result, the recently developed SPEI (Vicente-Serrano et al., 2010) was also introduced. In practice, both indices were highly correlated and only SPEI was used for burned area model building (Table 2).

2.6 Data Analysis

Climate and fire data were interpolated to a regular grid of 25 km resolution, representing a compromise between the 10 km resolution of the fire information and the ≃ 70 km horizontal resolution of ERA-Interim data. For each pixel, we computed daily time series of climate predictors (except SPEI and SPI, which are monthly, Table 2) and burned area. For the burned area models, the total monthly burned areas were calculated for each pixel and the climatic predictors were monthly averaged.

NHESSD
1, 4891–4924, 2013

We tested two different algorithms for model development: generalized linear models (GLM, McCullagh and Nelder, 1989) and multivariate adaptive regression splines (MARS, Friedman, 1991). On the one hand, GLMs constitute a parametric method widely used, thus constituting an adequate benchmarking method. On the other hand, MARS is a non–parametric method for regression. Unlike GLMs, MARS is able to model non-linearities in the data by approximating the underlying function through a set of adaptive piecewise linear regressions – known as *basis functions* – of the form:

$$y = \alpha_o + \sum_{k=1}^{K} \alpha_k b_k(\boldsymbol{x}), \tag{1}$$

where the slope of each piecewise $b_k(\boldsymbol{x})$ can change in a set of points z_{ki}, $i = 1, \ldots, m_k$, called knots. The popularity of this technique is due to the efficient optimization procedure used for the iterative search for basis functions and knots.

A comparative study of both MARS and GLM in the context of binary response predictions is done in Bedia et al. (2011, 2013). In both cases, the presence of redundant (highly correlated) predictors may introduce inconsistencies in variable importance estimates (see Sects. 2.6.1 and 2.6.2). Thus, we first computed the pairwise-correlation matrix with all candidate explanatory variables averaged at the country level, and eliminated one of each pair attaining correlation coefficients (Spearman's ρ) greater than 0.7. We decided to preserve variable pairs below this threshold in order to avoid the loss of useful information. The resulting subset of explanatory variables is indicated by the asterisks in Table 2.

2.6.1 Fire occurrence models

We used generalized linear models (GLM) for fire occurrence model development, considering the logit link function for the binary response variable (fire/no fire), at a daily resolution. We selected GLMs after finding that model performance was similar in this case than with the use of the more sophisticated MARS approach.

In order to analyse the effect of spatial aggregation of data in the models, we tested two different approaches of spatial aggregation of the data:

- *Grid-box models*: A full matrix of occurrence/absence of fires was constructed for each phytoclimatic zone, considering all the grid-boxes encompassed within the zone and the full daily time series (Fig. 3a). This will be referred to as the *grid-box* approach hereafter.

- *Areal models*: Occurrence/no occurrence data were aggregated at the phytoclimatic zone level, considering as occurrences all days in which at least one fire at one grid box took place, and absences to those days in which no fire took place at any of the grid boxes (Fig. 3c). This will be referred to as the *areal* approach hereafter.

In order to test the sensitivity of the models to fire size, we set different burned area thresholds for occurrence definition: 0.1, 1, 10 and 100 ha. As a result, only fires above the corresponding area thresholds were computed as occurrences.

Fire occurrence models were trained using all occurrence samples and fire absences randomly chosen in an equal number to the fire occurrences, thus using balanced datasets for model training to avoid an artificial inflation of model skill (see, e.g.: Manel et al., 2001; McPherson et al., 2004). For the grid-box model training, fire absences were sampled only from those days in which no fires occurred in any of the grid-boxes of the phytoclimatic zone (i.e., those rows of matrix in Fig. 3a in which all values are equal to zero), and this process was repeated 100 times in order to get a confidence interval of the sampling error. We then tested the resulting models using a random sample containing all possible cases. We undertook a one-year out cross-validation procedure, using 18 yr for training and the remaining one for testing, repeating this process 19 times, exactly one per year. From the resulting probabilistic predictions (see Fig. 3b and d for grid-box/areal probabilistic model predictions respectively) we computed the area under the receiver-operating characteristic curve (ROC skill area, RSA hereafter), which provides a quantitative measure of model skill (Swets, 1988). The possible range of RSA is [0,1]. Zero skill is indicated by RSA = 0.5, when the ROC lies along the positive diagonal, whereas RSA = 1.0 corresponds to a perfect skill. A RSA value below 0.5 corresponds to a ROC curve below the diagonal, indicating the same level of discrimination capacity as if it were reflected about the diagonal, but wrongly calibrated (Jolliffe and Stephenson, 2003). In order to compute the predicted fire frequencies, the probabilistic model predictions were converted into a binary prediction using two different approaches for decision threshold determination (both are illustrated in the right hand vertical plots of Fig. 3b and c for the grid-box/areal models):

- A global fixed probability threshold was determined by calculating the likelihood ratio of fire occurrence as given by the observations, and then applied to the full vector of predictions. This approach will be termed as *global threshold* hereafter.
- A monthly-varying threshold, corresponding to the likelihood ratio of fire occurrence as given by the observation, conditioned to the month. As a result, 12 different decision thresholds were obtained for each month of the year, which were applied to the predictions of the corresponding month to obtain the binary prediction. This threshold is referred to as *monthly threshold* in the following.

In order to estimate variable importance in the context of logistic regression, we applied the method of hierarchical partitioning, by which the independent effect of each variable is calculated by comparing the fit of all models containing a particular variable to the fit of all nested models lacking that variable (Chevan and Sutherland, 1991). For instance, for variable X_1, its importance I would be calculated as follows:

$$I_{x1} = \sum_{i=0}^{k-1} \frac{\sum (r^2_{y,X_1X_h} - r^2_{y,X_h}) / \binom{k-1}{i}}{k} \quad (2)$$

where X_h is any subset of i predictors from which X_1 is excluded. As a result, the variance shared by two or more correlated predictors can be partitioned into the variance

Discussion Paper | Discussion Paper | Discussion Paper | Discussion Paper |

NHESSD

1, 4891–4924, 2013

Modelling fire frequency and area burned in Spain

J. Bedia et al.

attributable to each predictor. This method provides a robust assessment of variable importance and has been shown to outperform other methods used for variable importance estimation in the context of regression analysis (Murray and Conner, 2009).

2.6.2 Burned area models

For the burned area models, we aggregated both fire and climate data in a monthly basis (1990–2008, $N = 228$ months). We used MARS as modelling algorithm because it performs well in the presence of outlying observations, as it is the case of large, infrequent fires. For this reason, it has been used in previous studies for modelling burned area (see e.g., Balshi et al., 2009; Amatulli et al., 2013).

In order to obtain robust estimates of model performance, we carried out a Leave-One-Out Cross Validation procedure (LOOCV) to compute the error (Michaelsen, 1987). LOOCV is a resampling technique in which $n-1$ instances out of the total of n, are used as the training dataset and the remaining one is used for testing. The procedure is repeated n times, one per observed instance, producing a more precise estimation of the classification accuracy. The method assumes that each sample is independent, so prior to its application we constructed autocorrelation plots of the monthly burned areas. We found a slight autocorrelation (maximum of 0.26) at some phytoclimatic types that resulted significant at the $\alpha = 0.05$ level. However, time series with autocorrelation of 0.25 or less will have an effective sample size at least of 90 % of the original sample size (Michaelsen, 1987), and thus it can be considered that this does not produce any measurable effect on the LOOCV estimates.

For variable importance estimation in the context of MARS, we looked at the reductions in the Generalized Cross–Validation estimate of error (GCV) in the selection routine performed by the MARS algorithm (Kuhn, 2010). The GCV is reduced each time a new variable is entered into the model. The accumulated reductions in GCV can be used as an estimate of variable importance, a value that is scaled to have a maximum of 100 and a minimum of zero (this minimum is reached when the variable is not used at all, or produces positive changes in GCV).

All the analyses were conducted in the R language and environment for statistical computing (R Core Team, 2013). The hierarchical partitioning was undertaken using the R package `hier.part` (Walsh and Mac Nally, 2013). For the MARS models, we used the implementation of the algorithm included in the R package `earth` (Milborrow, 2013). The drought indices SPI and SPEI were computed using the R package `SPEI` (Beguería and Vicente-Serrano, 2013).

3 Results and discussion

3.1 Fire regimes of the different phytoclimatic regions

We found two contrasting fire regimes in terms of area burned and number of fires across phytoclimatic zones: one characterized by a bimodal annual pattern, and another one exhibiting an unimodal annual cycle, with the fire season concentrated in the summer months (Fig. 2). The first case corresponds to the phytoclimatic types under the Atlantic influence (10–11–12 and 13–14–15), with two peaks of fire activity in March and August. These regions are characterized by temperate and wet conditions during most of the year, and also by relatively low fire danger conditions. In spite of the less suitable conditions for fire activity of these regions, there is a high number of fire records and also large burned areas. With this regard, previous studies highlight the strong influence that humans exert on fire regimes, and how fire incidence can be greatly enhanced for this reason even when climate conditions are not the most favourable (Vázquez et al., 2002). On the other hand, in the remaining phytoclimatic zones, belonging to the Mediterranean climate, fire activity is concentrated in the summer months and exhibit a marked unimodal annual cycle, coincident with the most favourable climatological conditions for fire.

3.2 Fire occurrence model performance and fire frequency results

Most phytoclimatic zones attained good model performance, and only zones 2–3, 10–11–12 and 13–14–15 yielded RSA values below 0.7 (Table 3). In terms of RSA, the models attained higher skills with increasing burned area thresholds, showing that the fire weather predictors used are more sensitive to the detection of larger fires than to smaller ones, being the latter not so closely dependent on favourable climate conditions for their occurrence. In all cases, the sampling error related to the random selection of days without fires was very low.

However, the good model skills are not directly linked to a good reproducibility of observed fire frequencies when working at the grid-box scale. With this regard, all models tended to a large overestimation of fire occurrence at this spatial scale, because all events of high danger potential are given a high probability of occurrence, in close relationship with the annual cycle of fire-weather danger (Fig. 3b). However, this effect is overridden when considering a larger spatial aggregation unit, because the probability of having at least one fire in a larger region when the conditions are favourable is much higher. This is illustrated in the observed and predicted fire occurrences/probabilities in Fig. 3c and d, evidencing the adequacy of the phytoclimatic zones defined as spatial aggregation units. As a result of areal aggregation, the predicted and observed magnitudes of fire frequencies are directly comparable (Fig. 4), attaining high correlation coefficients for some phytoclimatic zones (Table 4). Furthermore, the similar fire regimes of some phytoclimatic zones (Fig. 2) suggests the possibility of further aggregation into larger spatial units, leaving the door opened to the eventual improvement of model results. In the same vein, due to the marked seasonality of the fire danger potential, the seasonal adjustment of the probability threshold for case classification yielded in most occasions similar or better results than the global probability threshold (e.g. in phytoclimatic zones 2–3, 6, 9, 10–11–12, Table 4 and Fig. 4).

Variable importance assessment revealed in general that FWI and temperature are the chief climatic controls of fire occurrence, followed by other drought-related components

NHESSD
1, 4891–4924, 2013

of the FWI system (DC, FFMC). For the sake of conciseness, the results for the occurrence models are illustrated for the 10 ha burned area threshold models, although very similar results were obtained for the remaining burned area thresholds (Fig. 6).

3.2.1 Burned area models

Burned area was modelled with uneven accuracy depending on the phytoclimatic zone considered. The climatic predictors used as explanatory variables in the models provided an added explained variation when compared against a simple model incorporating only the annual cycle (respectively denoted as *clim* and *month* in Table 6), and therefore the skill of the models can not be solely attributed to the seasonal cycle of the fire danger predictors. The best result was attained in phytoclimatic zone 9 ($R^2 = 0.61$). In general terms, our results are comparable to previous analyses performed at a similar temporal scale (Amatulli et al., 2013). These authors also found considerable variability in model performance among different European countries, in a similar way as we find them across phytoclimatic regions in Spain. The reasons behind the idiosyncratic results of burned area models may lie in the presence of outlying observations (i.e. very large exceptional fires, see e.g. Trigo et al., 2006), and the influence of other landscape and anthropogenic factors beyond the explanatory ability of the climatic drivers in some regions (Viedma et al., 2006; Costa et al., 2011). Similarly, high fire danger situations may not directly translate into large burned areas; for instance, burned area may result less predictable in areas with complex topography (Balshi et al., 2009), such as the northern parts of Spain. Furthermore, the effectiveness of fire suppression schemes may prevent from the occurrence of large fires in situations of high fire danger (see e.g. Turco et al., 2013). Further complications arise from the interpretation of fire history from records of burned area alone (see e.g. Niklasson and Granstrom, 2000). For instance, the same burned area might be the result of a few large fires, more closely linked to exceptional high danger conditions – this is illustrated by the good model performance of the large fire occurrence models, as depicted in Table 3 –, or of many small fires which may be more related to anthropogenic factors – as indicated by the lower performance of these models in the Atlantic regions 10–11–12 and 13–14–15 in Table 3 –.

As a result, the predictability of burned area resulted unstable, and in most zones we obtained non-significant inter-annual burned area cross-correlations between observed and predicted time series, with the presence of some outlying predictions (as in zone 4, year 1994) and even a spurious negative significant correlation in the case of phytoclimatic zone 2–3 (Fig. 5). Nevertheless, it is remarkable the good reproducibility of annual burned areas attained in phytoclimatic zone 6, and to a lesser extent in zones 9 and 10–11–12, although the results of annual fire frequencies are much more robust and consistent across zones (Table 4).

Regarding the climatic controls of burned area, the drought index SPEI was an important predictor in some phytoclimatic zones (Table 5), notably in the model of zone 9, which is the one attaining the highest explained variance (Table 6), and also performed well in the representation of annual burned areas (Spearman's $\rho = 0.56$, Fig. 5). On the contrary, SPEI was not selected by the models in other zones (6, 7–8, 10–11–12), suggesting that the effect of drought on fire size is very different depending on the vegetation types. Temperature, DC, FWI and FFMC were selected by all models with varying importance, although all models always selected a FWI system component and/or temperature as the most important variables, indicating the importance of these predictors at the monthly scale for the estimation of burned area. In the particular case of zone 6 – which obtained the highest inter-annual correlation with observed burned area – the most important explanatory variables were temperature, and the FWI components DC and FFMC.

4 Conclusions

Our results support the use of ERA-Interim reanalysis and the FWI system for fire modelling applications in Spain, provided an adequate temporal and spatial scale of data analysis and interpretation. Grid-box models of fire occurrence yielded in general

NHESSD
1, 4891–4924, 2013

good model skill in terms of RSA, although this fact does not translate directly into a good reproducibility of fire frequencies, due to the inherent tendency of the method to over-estimate fire occurrence. Nonetheless, the annual cycle was adequately modelled regardless of the distributional characteristics of the different annual fire regimes of each phytoclimatic zone. Temperature and some components of the FWI system (FWI itself and DC and FFMC in particular) were the most important predictors of fire occurrence.

Areal models yielded accurate predictions of the inter-annual fire frequency series, showing that the aggregation of the data into larger spatial units is needed for an adequate analysis the climatic drivers of fires, and that the phytoclimatic zones used in this study constitute representative units of the climate-fire relationship, without prejudice to the application of other convenient aggregation units as long as this representativeness is preserved, such as the different phytoclimatic/bioclimatic classifications available at different scales throughout the world, or other type of classifications based on fire regime characteristics (see e.g. Archibald et al., 2013).

We attained fair burned area model results for some phytoclimatic zones, although most of them failed to adequately reproduce the inter-annual burned area series, with some exceptions. In all cases, burned areas were mostly explained by temperature and drought-related indices bearing some sort of "memory" on the antecedent conditions, such as the FWI system components DC and FFMC, or the recently developed drought index SPEI. As a result, the practical application of burned area models for certain aims, such as the prediction of future burned area scenarios, poses important limitations, being the fire frequency models more robust to this aim.

Acknowledgements. We are grateful to Pilar Martín and Israel Gómez for their help with fire data gathering. The research leading to these results has received funding from the European Union's Seventh Framework Programme (FP7/2007-2013) under grant agreement 243888 (FUME Project).

References

Allué, J.: Atlas Fitoclimático de España. Taxonomías, Tech. rep., Instituto Nacional de Investigaciones Agrarias, Ministerio de Agricultura, Pesca y Alimentación, Madrid, Spain, 221 pp., 1990. 4894, 4895

Amatulli, G., Camia, A., and San-Miguel-Ayanz, J.: Estimating future burned areas under changing climate in the EU-Mediterranean countries, Sci. Total Environ., 450–451, 209–222, 2013. 4901, 4904

Archibald, S., Lehmann, C. E. R., Gomez-Dans, J. L., and Bradstock, R. A.: Defining pyromes and global syndromes of fire regimes, Proc. Natl. Aca. Sci. USA, 110, 6442–6447, 2013. 4906

Balshi, M., McGuire, A., Duffy, P., Flannigan, M., Walsh, J., and Melillo, J.: Assessing the response of area burned to changing climate in wester boreal North America using a Multivariate Adaptive Regression Splines (MARS) approach, Global Change Biol., 15, 578–600, 2009. 4901, 4904

Barbati, A., Arianoutsou, M., Corona, P., De Las Heras, J., Fernandes, P., Moreira, F., Papageorgiou, K., Vallejo, R., and Xanthopoulos, G.: Post-fire forest management in southern Europe: a COST action for gathering and disseminating scientific knowledge, Iforest-Biogeosciences and Forestry, 3, 5–7, 2010. 4893

Bedia, J., Busqué, J., and Gutiérrez, J. M.: Predicting plant species distribution across an alpine rangeland in northern Spain: a comparison of probabilistic methods, Appl. Veg. Sci., 14, 415–432, 2011. 4898

Bedia, J., Herrera, S., Gutiérrez, J. M., Zavala, G., Urbieta, I. R., and Moreno, J. M.: Sensitivity of fire weather index to different reanalysis products in the Iberian Peninsula, Nat. Hazards Earth Syst. Sci., 12, 699–708, doi:10.5194/nhess-12-699-2012, 2012. 4894, 4896

Bedia, J., Herrera, S., and Gutiérrez, J. M.: Dangers of using global bioclimatic datasets for ecological niche modeling. Limitations for future climate projections, Global Planet. Change, 107, 1–12, 2013. 4898

Beerling, D. J. and Osborne, C. P.: The origin of the savanna biome, Global Change Biol., 12, 2023–2031, 2006. 4893

Beguería, S. and Vicente-Serrano, S. M.: SPEI: Calculation of the Standardised Precipitation-Evapotranspiration Index, available at: http://CRAN.R-project.org/package=SPEI, r package version 1.3, 2013. 4902

NHESSD
1, 4891–4924, 2013
Modelling fire frequency and area burned in Spain
J. Bedia et al.

Bond, W., Woodward, F., and Midgley, G.: The global distribution of ecosystems in a world without fire, New Phytologist, 165, 525–537, 2005. 4893

Bowman, D. M. J. S., Balch, J. K., Artaxo, P., Bond, W. J., Carlson, J. M., Cochrane, M. A., D'Antonio, C. M., DeFries, R. S., Doyle, J. C., Harrison, S. P., Johnston, F. H., Keeley, J. E., Krawchuk, M. A., Kull, C. A., Marston, J. B., Moritz, M. A., Prentice, I. C., Roos, C. I., Scott, A. C., Swetnam, T. W., van der Werf, G. R., and Pyne, S. J.: Fire in the Earth System, Science, 324, 481–484, 2009. 4893

Chevan, A. and Sutherland, M.: Hierarchical Partitioning, The American Statistician, 45, 90–96, 1991. 4900

Costa, L., Thonicke, K., Poulter, B., and Badeck, F.-W.: Sensitivity of Portuguese forest fires to climatic, human, and landscape variables: subnational differences between fire drivers in extreme fire years and decadal averages, Reg. Environ. Change, 11, 543–551, 2011. 4904

Dee, D. P., Uppala, S. M., Simmons, A. J., Berrisford, P., Poli, P., Kobayashi, S., Andrae, U., Balmaseda, M. A., Balsamo, G., Bauer, P., Bechtold, P., Beljaars, A. C. M., van de Berg, L., Bidlot, J., Bormann, N., Delsol, C., Dragani, R., Fuentes, M., Geer, A. J., Haimberger, L., Healy, S. B., Hersbach, H., Hólm, E. V., Isaksen, L., Kållberg, P., Köhler, M., Matricardi, M., McNally, A. P., Monge-Sanz, B. M., Morcrette, J., Park, B., Peubey, C., de Rosnay, P., Tavolato, C., Thépaut, J.-N., and Vitart, F.: The ERA-Interim reanalysis: configuration and performance of the data assimilation system, Q. J. R. Meteorol. Soc., 137, 553–597, 2011. 4896, 4913

Friedman, J. H.: Multivariate adaptive regression splines, Ann. Stat., 19, 1–67, 1991. 4898

Hardy, C.: Wildland fire hazard and risk: Problems, definitions, and context, FOREST ECOLOGY AND MANAGEMENT, 211, 73–82, Symposium on Relative Risk Assessments for Decision-Making Related to Uncharacteristic Wildfire, Portland, OR, NOV, 2003, 2005. 4893

Jolliffe, I. and Stephenson, D. (Eds.): Forecast Verification. A Practitioner's guide in Atmospheric Science, Wiley, Chichester, England, 2003. 4900

Keeley, J.: Impact of antecedent climate on fire regimes in coastal California, Int. J. Wildland Fire, 13, 173–182, 2004. 4893

Koutsias, N., Arianoutsou, M., Kallimanis, A., Mallinis, G., Halley, J., and P., D.: Where did the fires burn in Peloponnisos, Greece, the summer of 2007? Evidence for a synergy of fuel and weather, Agr. Forest Meteorol., 156, 41–53, 2012. 4893

Kuhn, M.: Variable importance using the caret package, The Comprehensive R Archive Network, available at: http://cran.open-source-solution.org/web/packages/caret/vignettes/caretVarImp.pdf (last access: 16 September 2013), 2010. 4901

Littell, J., McKenzie, D., Peterson, D., and Westerling, A.: Climate and wildfire area burned in western U.S. ecoprovinces, 1916–2003, Ecol. Appl., 19, 1003–1021, 2009. 4897

Manel, S., Williams, H. C., and Ormerod, S. J.: Evaluating presence-absence models in ecology: the need to account for prevalence, J. Appl. Ecol., 38, 921–931, 2001. 4899

Marlon, J. R., Bartlein, P. J., Carcaillet, C., Gavin, D. G., Harrison, S. P., Higuera, P. E., Joos, F., Power, M. J., and Prentice, I. C.: Climate and human influences on global biomass burning over the past two millennia, Nat. Geosci., 1, 697–702, 2008. 4893

McCullagh, P. and Nelder, J.: Generalized linear models, Chapman & Hall, London, 1989. 4898

McKee, T., Doesken, J., and Kleist, J.: The relationship of drought frecuency and duration to time scales, in: Proceedings of the Eight Conf. On Applied Climatology, Anaheim, CA, American Meteorological Society, 179–184, 1993. 4897, 4913

McPherson, J., Jetz, W., and Rogers, D.: The effects of species' range sizes on the accuracy of distribution models: ecological phenomenon or statistical artefact?, J. Appl. Ecol., 41, 811–823, 2004. 4899

Mérida, J., Primo, E., Eleazar, J., and Parra, J.: Las Bases de Datos de Incendios Forestales como herramienta de planificación: utilización en España por el Ministerio de Medio Ambiente, in: Proceedings of the 4th International Wildland Fire Conference, Sevilla, Spain, 13–18 May 2007, edited by: Organismo Autónomo de Parques Nacionales, M. d. M. A., available at: http://www.fire.uni-freiburg.de/sevilla-2007/contributions/doc/cd/SESIONES_TEMATICAS/ST4/Merida_et_al_SPAIN_DGB.pdf (last access: 9 September 2013), 2007 (in Spanish). 4895

Meyn, A., White, P. S., Buhk, C., and Jentsch, A.: Environmental drivers of large, infrequent wildfires: the emerging conceptual model, Prog. Phys. Geogr., 31, 287–312, 2007. 4894

Meyn, A., Schmidtlein, S., Taylor, S., Girardin, M., Thonicke, K., and Cramer, W.: Spatial variation of trends in wildfire and summer drought in British Columbia, Canada, 1920–2000, Int. J. Wildland Fire, 19, 272–283, 2010. 4897

Michaelsen, J.: Cross-Validation in Statistical Climate Forecast Models, J. Clim. Appl. Meteorol., 26, 1589–1600, 1987. 4901

Milborrow, S.: earth: Multivariate Adaptive Regression Spline Models, available at: http://CRAN.R-project.org/package=eart (last access: 16 September 2013), R package version 3.2-6, 2013. 4902

Murray, K. and Conner, M.: Methods to quantify variable importance: implications for the analysis of noisy ecological data, Ecology, 90, 348–355, 2009. 4901

Niklasson, M. and Granstrom, A.: Numbers and sizes of fires: Long-term spatially explicit fire history in a Swedish boreal landscape, Ecology, 81, 1484–1499, 2000. 4904

Pausas, J.: Changes in fire and climate in the Eastern Iberian Peninsula (Mediterranean Basin), Climatic Change, 63, 337–350, 2004. 4893

Pausas, J. G. and Paula, S.: Fuel shapes the fire-climate relationship: evidence from Mediterranean ecosystems, Global Ecol. Biogeogr., 21, 1074–1082, 2012. 4893

Pereira, M., Trigo, R., da Camara, C., Pereira, J., and Leite, S.: Synoptic patterns associated with large summer forest fires in Portugal, Agr. Forest Meteorol., 129, 11–25, 2005. 4893, 4897

R Core Team: R: A Language and Environment for Statistical Computing, R Foundation for Statistical Computing, Vienna, Austria, available at: http://www.R-project.org/ (16 September 2013), 2013. 4902

Rivas Martínez, S.: Mapa de las Series de Vegetación de la Península Ibérica, Tech. rep., ICONA. Ministerio de Agricultura, Pesca y Alimentación, 1987. 4895

Stocks, B., Lawson, B., Alexander, M., Van Wagner, C., McAlpine, R., Lynham, T., and Dube, D.: The Canadian Forest Fire Danger Rating System – An Overview, For. Chron., 65, 450–457, 1989. 4896

Swets, J.: Measuring the accuracy of diagnostic systems, Science, 240, 1285–1293, 1988. 4899

Trigo, R., Pereira, J., Pereira, M., Mota, B., Calado, T., DaCamara, C., and Santo, F.: Atmospheric conditions associated with the exceptional fire season of 2003 in Portugal, Int. J. Climatol., 26, 1741–1757, 2006. 4904

Turco, M., Llasat, M., von Hardenberg, J., and Provenzale, A.: Impact of climate variability on summer fires in a Mediterranean environment (northeastern Iberian Peninsula), Climatic Change, 116, 665–678, doi:10.1007/s10584-012-0505-6, 2012. 4893

Turco, M., Llasat, M. C., Tudela, A., Castro, X., and Provenzale, A.: Brief communication Decreasing fires in a Mediterranean region (1970–2010, NE Spain), Nat. Hazards Earth Syst. Sci., 13, 649–652, doi:10.5194/nhess-13-649-2013, 2013. 4904 van Wagner, C. E.: Development and structure of the Canadian Forest Fire Weather Index, Forestry Tech. Rep. 35, Canadian Forestry Service, Ottawa, Canada, 1987. 4896, 4913

Vázquez, A., Pérez, B., Fernández-González, F., and Moreno, J.: Recent fire regime characteristics and potential natural vegetation relationships in Spain, J. Veg. Sci., 13, 663–676, 2002. 4902

Vicente-Serrano, S., Beguería, S., and López-Moreno, J.: A Multi-scalar drought index sensitive to global warming: The Standardized Precipitation Evapotranspiration Index – SPEI, J. Climate, 7, 1696–1718, doi:10.1175/2009JCLI2909.1, 2010. 4897, 4913

Viedma, O., Moreno, J. M., and Rieiro, I.: Interactions between land use/land cover change, forest fires and landscape structure in Sierra de Gredos (Central Spain), Environ. Conservation, 33, 212–222, 2006. 4904

Walsh, C. and Mac Nally, R.: hier.part: Hierarchical Partitioning, available at: http://CRAN.R-project.org/package=hier.part (last access: 16 September 2013), r package version 1.0-4, 2013. 4902

NHESSD
1, 4891–4924, 2013

Modelling fire frequency and area burned in Spain

J. Bedia et al.

Table 1. The spatial distribution of the phytoclimatic types is displayed in Fig. 1. Note that the area is referred to each phytoclimatic type.

General Phytoclim. types	Potential Vegetation	Veg. Subtypes	Phytoclim types	Area (kha)
Arid	*Ziziphus lotus*, *Periploca laevigata*	III(IV)	1	25.5
Mediterranean	*Pistacia lentiscus*, *Olea europaea* var. *sylvestris*, *Quercus coccifera*, *Q. ilex rotundifolia*, *Q. ilex ilex*	IV(III)	2	1348.6
		IV(VII)	3	3191.5
		IV1	3	
		IV2	4	3591
		IV3	5	4121.6
		IV4	6	8776.2
		IV(VI)1	7	4691.7
		IV(VI)2	8	865.4
Nemoral	*Quercus faginea*, *Q. pyrenaica*, *Q. ilex ilex*, *Q. humilis*, *Q. robur*, *Fagus sylvatica*	VI(IV)1	9	10621.3
		VI(IV)2	10	2955.7
		VI(IV)3	11	196.7
		VI(IV)4	12	550.1
		VI(VII)	13	1974.2
		VI(V)	14	3868.2
		VI	15	1179.7
Oro-boreal	*Pinus sylvestris*, *P. uncinata*, *Q. humilis*, *Fagus sylvatica*, sub-alpine and alpine grasslands	VIII(VI)	16	1481.9
		X(VIII)	17	326.7
		X(IX)1	18	117.5
		X(IX)2	18	

NHESSD
1, 4891–4924, 2013

Title Page
Abstract | Introduction
Conclusions | References
Tables | Figures
◀| |▶
◀ ▶
Back | Close
Full Screen / Esc
Printer-friendly Version
Interactive Discussion

NHESSD
1, 4891–4924, 2013

Modelling fire frequency and area burned in Spain

J. Bedia et al.

Table 2. Summary of predictors tested in this study for fire model building. After checking for redundancy, a final subset of weakly-correlated variables was used for model building, marked with an asterisk (Note that SPEI is a monthly indicator, and therefore it was only used as predictor for the burned area models). [ET0 = potential evapotranspiration].

	Variable	Code	Input vars.	T. aggreg	Reference
Climatic variables	*Temperature (12:00 UTC)	T_12	–	instantaneous	Dee et al. (2011)
	Rel. humidity (12:00 UTC)	H_12	Specific H_12,T_12	instantaneous	
	*Precipitation	P	–	24h accum.	
	*Wind velocity (12:00 UTC)	W_12	–	instantaneous	
FWI system components	*Fine fuel moisture code	FFMC	T_12,H_12,P,W_12	daily	van Wagner (1987)
	Duff moisture code	DMC	T_12,H_12,P	daily	
	*Drought code	DC	T_12,P	daily	
	Initial spread index	ISI	FFMC,W_12	daily	
	Buildup index	BUI	DMC,DC	daily	
	*Fire Weather index	FWI	ISI,BUI	daily	
	Daily severity rating	DSR	FWI	daily	
Drought indices	Std. precip. index	SPI	*P*	monthly	McKee et al. (1993)
	*Std. precip.-evap. index	SPEI	*P*, ET0	monthly	Vicente-Serrano et al. (2010)

Table 3. ROC skill area (RSA) attained by the fire occurrence models for each phytoclimatic zone. The quantilic range (97.5–2.5 %) after 100 randomly selected fire absences is indicated in parenthesis. Results are presented for the different burned area thresholds used for fire occurrence definition.

Phyt. zone	0.1 ha	1 ha	10 ha	100 ha
2–3	0.67(0.01)	0.68(0.02)	0.73(0.04)	0.77(0.10)
4	0.75(0.01)	0.77(0.01)	0.79(0.03)	0.80(0.06)
5	0.78(0.01)	0.80(0.01)	0.83(0.02)	0.85(0.06)
6	0.75(0.01)	0.76(0.01)	0.80(0.02)	0.84(0.04)
7–8	0.73(0.01)	0.75(0.01)	0.79(0.03)	0.80(0.08)
9	0.68(0.01)	0.70(0.01)	0.76(0.02)	0.82(0.04)
10–11–12	0.67(0.01)	0.66(0.01)	0.67(0.01)	0.74(0.04)
13–14–15	0.62(0.00)	0.58(0.01)	0.57(0.01)	0.66(0.03)

NHESSD
1, 4891–4924, 2013

Modelling fire frequency and area burned in Spain

J. Bedia et al.

Table 4. Spearman's ρ cross–correlation coefficients between the observed and predicted annual fire frequencies, determined using the global and monthly probability thresholds. The results correspond to both the the grid-box and areal models. The number of grid-boxes comprising each phytoclimatic zone are indicated by the *N grid-boxes* column (see the legend of Fig. 1 for a visual indication of their size). The results are presented for the different burned area thresholds used to define fire occurrence/absence. n.s. indicates that the correlation was not significant at the 95 % confidence interval.

Phytoclim.	N grid-boxes	P. thresh.	Grid-box Models				Areal Models			
			0.1 ha	1 ha	10 ha	100 ha	0.1 ha	1 ha	10 ha	100 ha
2–3	77	Global	n.s.	n.s.	n.s.	n.s.	n.s.	n.s.	n.s.	n.s.
		Monthly	n.s.	n.s.	n.s.	n.s.	0.74	n.s.	n.s.	n.s.
4	57	Global	n.s.	n.s.	n.s.	n.s.	0.70	0.50	n.s.	n.s.
		Monthly	n.s.	n.s.	n.s.	n.s.	0.85	0.52	n.s.	n.s.
5	70	Global	n.s.	n.s.	0.61	0.50	0.53	0.59	0.56	0.56
		Monthly	n.s.	n.s.	0.43	n.s.	0.48	0.57	0.45	0.58
6	158	Global	n.s.	n.s.	0.39	0.58	0.83	0.70	0.40	0.40
		Monthly	n.s.	n.s.	n.s.	0.65	0.77	0.76	n.s.	n.s.
7–8	91	Global	n.s.	n.s.	n.s.	0.44	0.54	0.51	0.59	n.s.
		Monthly	n.s.	n.s.	n.s.	0.44	0.78	n.s.	0.40	n.s.
9	194	Global	0.41	n.s.	0.61	0.44	0.88	0.52	0.56	0.47
		Monthly	0.48	n.s.	0.48	n.s.	0.78	0.58	0.49	0.44
10–11–12	81	Global	0.67	n.s.	n.s.	n.s.	0.83	0.56	0.46	n.s.
		Monthly	0.60	n.s.	n.s.	n.s.	0.74	0.61	n.s.	n.s.
13–14–15	158	Global	0.60	0.64	0.48	n.s.	n.s.	n.s.	n.s.	n.s.
		Monthly	0.40	n.s.	n.s.	n.s.	n.s.	n.s.	n.s.	n.s.

NHESSD
1, 4891–4924, 2013

Table 5. Variable importance (GCV, in %) of each input variable ± standard deviation, (n = 228 LOOCV models). The percentage of LOOCV models including the variable is indicated in parenthesis. Variables not selected by the MARS algorithm are indicated by asterisks. Note that SPEI is not a candidate variable in the fire occurrence models.

Phytoclim.	T12	SPEI	W12	DC	FWI	Pr	FFMC
2–3	100 ± 0(100)	70 ± 13.6(97)	74 ± 15.8(100)	40 ± 9.9(97)	41 ± 7.3(98)	38 ± 9.8(99)	7 ± 24.6(16)
4	100 ± 0(100)	25 ± 5.7(93)	99 ± 1.2(100)	44 ± 8.6(100)	68 ± 5.8(97)	12 ± 19.4(22)	54 ± 7(100)
5	83 ± 16.6(100)	66 ± 11.3(100)	33 ± 9.8(99)	4 ± 17.6(41)	67 ± 23.5(85)	8 ± 13.3(24)	79 ± 25.9(100)
6	100 ± 0(100)	*	*	40 ± 3.6(100)	1 ± 7.7(7)	*	57 ± 3.1(100)
7–8	4 ± 21.4(11)	*	*	46 ± 6(100)	90 ± 4.7(90)	*	35 ± 8.5(100)
9	12 ± 9.6(97)	96 ± 14.1(99)	23 ± 13.7(100)	27 ± 12(100)	99 ± 7.2(100)	6 ± 30.4(19)	5 ± 9.4(45)
10–11–12	55 ± 15.8(100)	1 ± 14.3(4)	27 ± 9(72)	100 ± 0(100)	92 ± 15(100)	32 ± 15.5(92)	52 ± 4.7(100)
13–14–15	52 ± 7.1(100)	55 ± 5(99)	94 ± 9.2(100)	36 ± 11.1(100)	21 ± 18(99)	39 ± 14.4(98)	99 ± 5.4(100)

NHESSD
1, 4891–4924, 2013

Table 6. Explained variance (adjusted-R^2, observed *vs.* predicted) of the LOOCV models for area burned. The models including only the seasonal cycle (i.e. the month as the only explanatory variable) are indicated as *month*. The models using the climatic explanatory variables (Table 2) are indicated as *clim*.

Phytoclim. zone	*month*	*clim*
2–3	0.13	0.27
4	0.13	0.45
5	0.20	0.50
6	0.22	0.52
7–8	0.18	0.53
9	0.11	0.61
10–11–12	0.30	0.44
13–14–15	0.06	0.40

NHESSD
1, 4891–4924, 2013

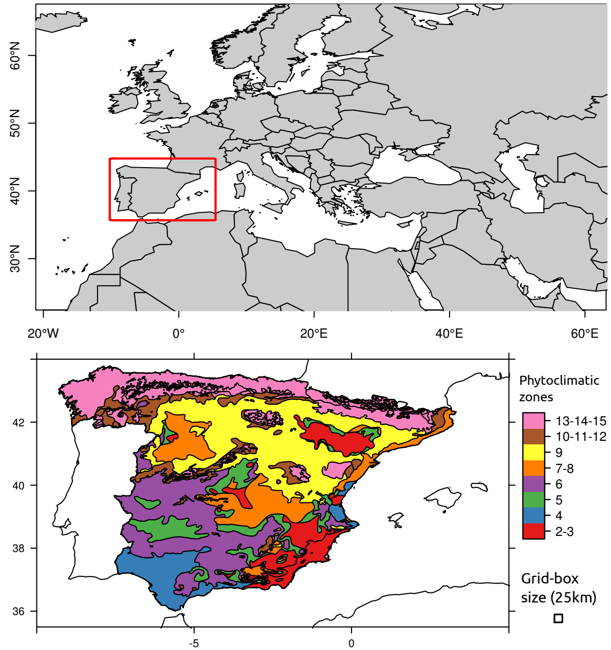

Fig. 1. Location of the study area. Colour divisions correspond to the different phytoclimatic areas used for the analysis after aggregation (see details in Sect. 2.2 and Table 1). The grid of analysis is also indicated.

NHESSD
1, 4891–4924, 2013

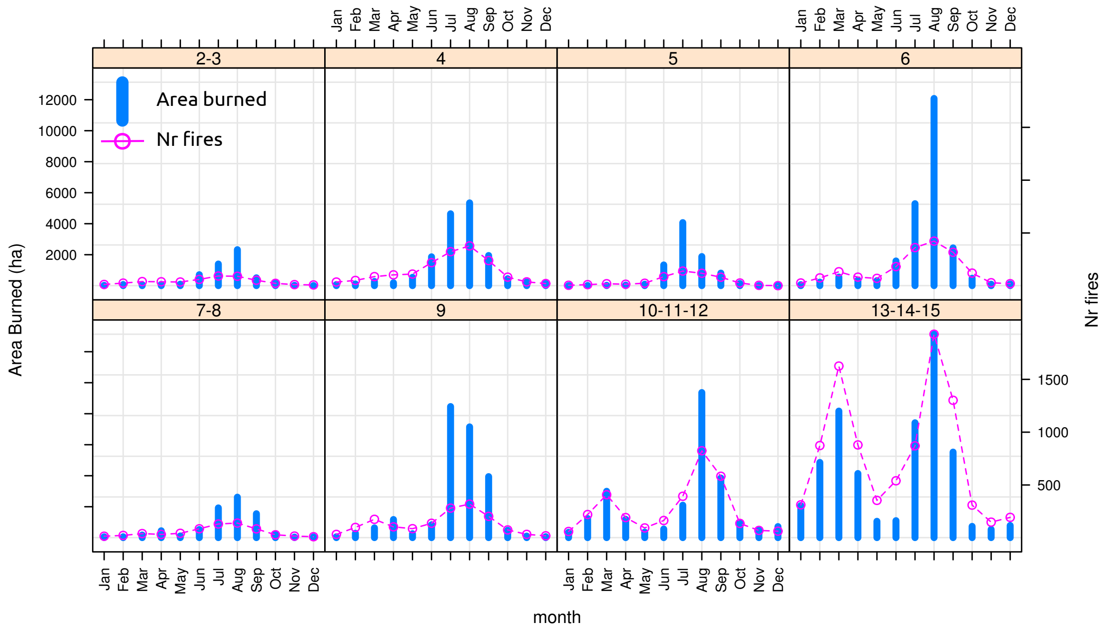

Fig. 2. Mean monthly area burned (vertical bars, main *y* axis) and mean number of fires (lines and dots, secondary *y* axis) recorded for the period 1990–2008 in Spain, at the different phyto-climatic regions.

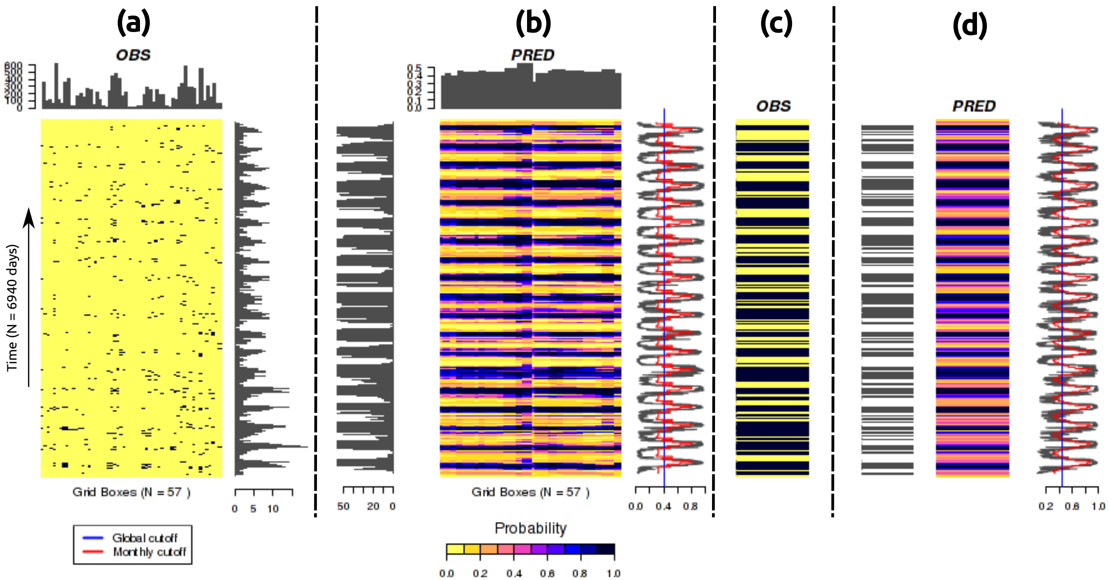

NHESSD
1, 4891–4924, 2013

Modelling fire frequency and area burned in Spain

J. Bedia et al.

Fig. 3. Observed and predicted data representation of fire occurrence considering both the grid-box **(a–b)** and areal **(c–d)** approaches. The example corresponds to the phytoclimatic zone 4, characterised by an unimodal annual fire regime, with a peak of fire activity in the aestival months (JJAS, Fig. 2). The panel on the left **(a)** represents the data matrix of the observed fires at the grid-box scale. Rows represent from bottom to top the time series of the analysis period (1990–2008, 6940 days). Columns correspond to the 25 km grid boxes belonging to the phytoclimatic type. Fire events (those above the threshold of 0.1ha of burnt area) are denoted by the blue lines. The bar plot on the right hand side of the matrix depicts the daily fire counts, and the bar plot on the top the total fire counts per pixel for the whole analysis period. Panel **(b)** represents the modelled fire occurrence. The central matrix corresponds to the predicted probabilities of fire occurrence for each day and for each grid box. The graph on the right hand side corresponds to the mean daily probabilities (grey line), and the two types of probability thresholds considered for case classification: the global probability threshold (blue line) and the monthly probability threshold (red line), which can take 12 different values, one for each month of the year. The resulting binary classification using the monthly probability threshold leads to the daily predicted fire counts presented in the left hand side bar plot. The bar plot on the top depicts the mean predicted probabilities for each grid box. The fire occurrence at the phytoclimatic zone level (areal approach) is represented in panel **(c)**. In this case, fire occurrence takes place when a fire occurs in at least one of the pixels belonging to that zone (note that this matrix has the same number of rows -days- than **(a)** and **(b)** but one single column, as all pixels integrating the area have been aggregated). Finally, panel **(d)** represents the predicted probabilities by the areal modelling approach. The time series of the daily predicted probabilities with the two probability thresholds are presented in the right hand side plot. The column on the left represents the resulting binary fire occurrence prediction (grey = occurrence, white=absence) using the monthly probability threshold.

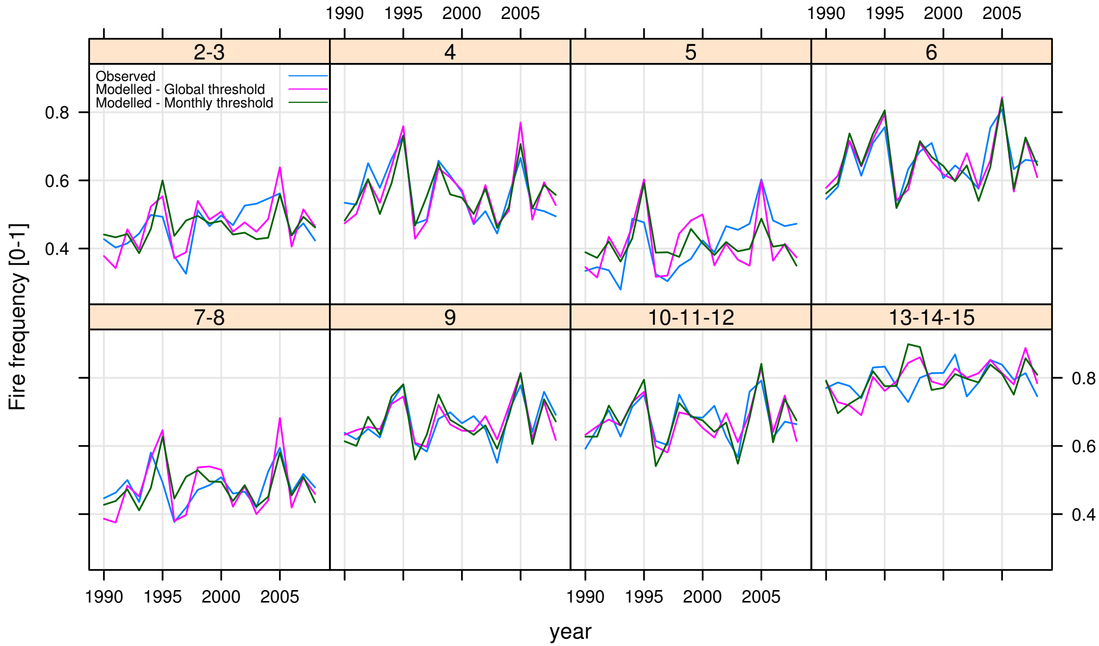

Fig. 4. Observed and 1-year-out cross-validated predicted annual fire frequencies at each phytoclimatic zone, considering the two different probability threshold values for case classification, according to the areal models and the burned area threshold of 0.1 ha. Cross-correlation values between observed and predicted series are presented in Table 4.

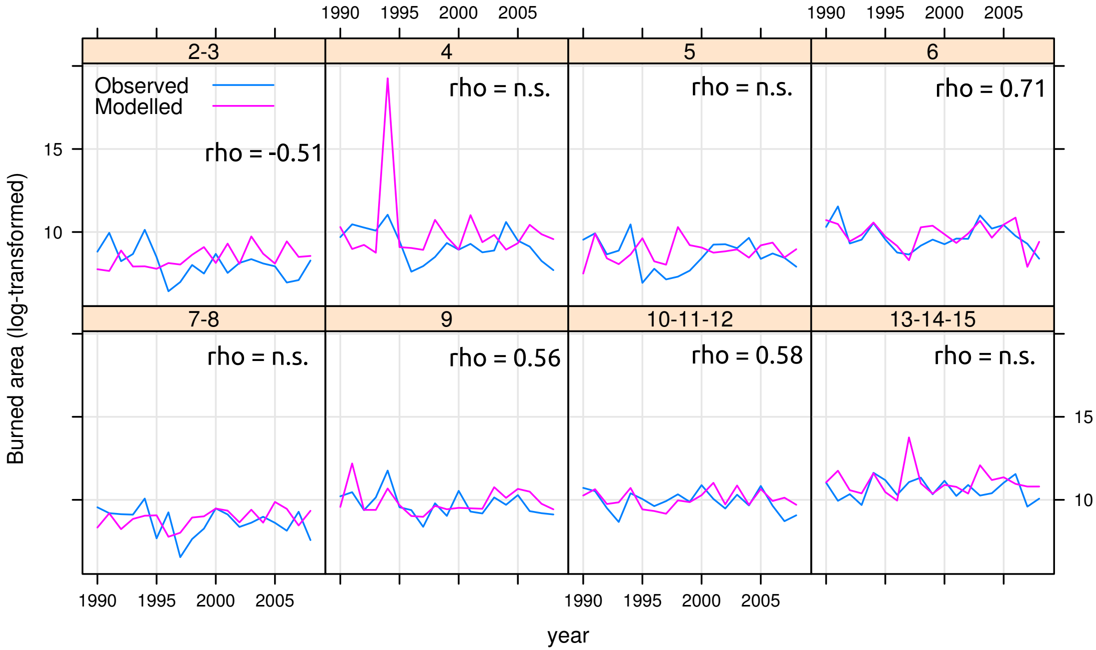

Fig. 5. Observed and cross-validated predicted annual burned areas at each phytoclimatic zone. Cross-correlation values (Spearman's ρ) between observed and predicted series are indicated in the panels (n.s. = non significant correlation at the 0.05 α level)

NHESSD
1, 4891–4924, 2013
Modelling fire frequency and area burned in Spain
J. Bedia et al.

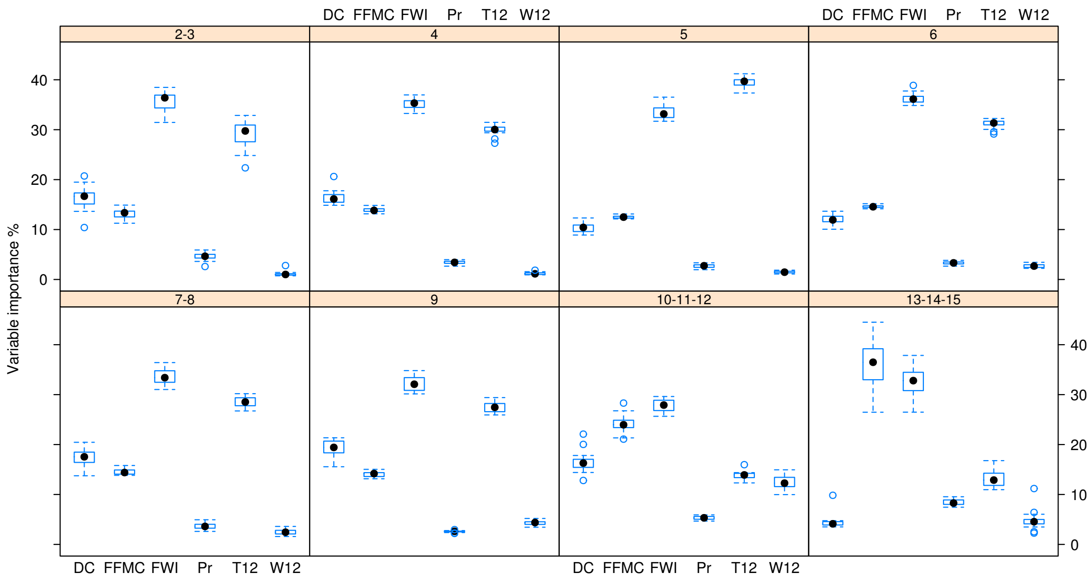

Fig. 6. Boxplots of variable importance (% of total explained variance) in the fire occurrence models for each phytoclimatic zone. The results presented correspond to the 10 ha burned area threshold. The interval ranges correspond to variable importance scores attained in each of the 19 one-year-out cross validation results (see Sect. 2.6.1 for details).

NHESSD
1, 4891–4924, 2013